

Origami Hexagon Deformations and Flip Graph

July 2020

Abstract

We studied the collection of configurations of an isolated hexagon consisting of six equilateral triangles around a vertex on the triangular lattice. We quantitatively characterized the moduli space of deformations near the flat state. The rational and integer points on the deformation surface joining with flip operations admit a consistent combinatorial structure.

Contents

1	Introduction	2
2	Configuration space of an origami hexagon	2
2.1	An isolated origami hexagon	2
2.2	Moduli space of deformations	3
3	Rational points on the hexagon configuration space	4
3.1	Interpretation of the projective space	4
3.2	Rational parametrization	5
3.3	Flip operation	6
4	Integer points and the flip graph	7
4.1	Flip graph	9
4.2	Mountain-valley classification	12
5	Pythagorean 4-tuples	14
5.1	Pythagorean graph	15
5.2	Connection to hexagon configuration	16
5.2.1	Flip operation	16
5.2.2	Pythagorean graph \mathcal{H} and hexagon flip graph \mathcal{G}	16

1 Introduction

By utilizing origami folding processes, researchers have been able to solve a wide range of engineering problems such as fabricating different robot morphologies [1] and manufacturing folding-based mechanisms [7]. Leveraging origami structures in this way requires an understanding of geometric and numerical properties of folding configurations. Given a crease or linkage pattern, it is natural to ask what the relations among fold angles without curving subplanes or breaking hinges are.

In this paper, we focused on an isolated origami hexagon. In Section 2, we parametrized the configuration space by six fold angles. Izmistiev reexamined the parametrization of the angles in a general four-bar linkage [6], which is regarded as a planar version of our topic. By applying second order approximation, we obtained the moduli space of deformations near the flat state with three degrees of freedom.

In Section 3, we discussed the rational parametrization, followed by the existence of six natural flip operations on the moduli space, corresponding to a local change at each of the six folds on the hexagon. A similar flip transformation for a planar quadrilateral is introduced in the Darboux' folding porism [5].

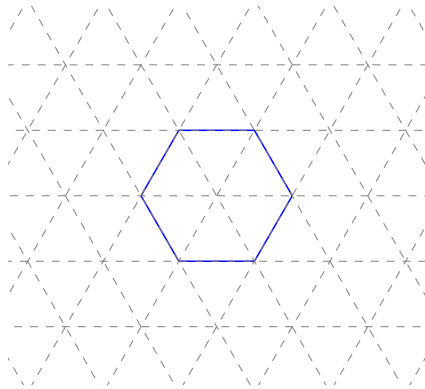
In Section 4, we created an acyclic directed graph from the action of these flip operations on integer-valued points. This flip graph is analogous to the Calkin–Wilf tree. We gave out closed formulas for the number of vertices on each level and the number of mountain-valley configurations among them. By generating the Markov transition matrix, we calculated the limiting distribution for mountain-valley configurations. In Section 5, the connection between Pythagorean 4-tuples and integer solutions is interpreted.

2 Configuration space of an origami hexagon

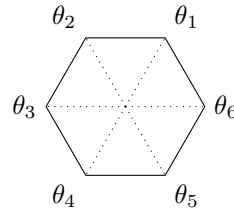
2.1 An isolated origami hexagon

An isolated origami hexagon consists of six equilateral triangles around a vertex on the triangular lattice, as shown in Figure 1a. Only considering the subplane marked inside the blue boundary, Figure 1b indicates the crease pattern of an oriented isolated origami hexagon.

We are interested in the massless configuration space of an oriented isolated origami hexagon, i.e. each face is allowed to pass through itself. See more configuration examples in Figure 2. In the following context, every origami hexagon refers to an oriented isolated origami hexagon.



(a) Hexagon on triangular lattices



(b) Isolated hexagon with parametrization

Figure 1: Origami hexagon

To understand the geometric classification problem for an origami hexagon, we parametrize its configuration collection by six fold angles,

$$(\theta_1, \theta_2, \dots, \theta_6), \theta_i \in \mathbb{R}/2\pi\mathbb{Z},$$

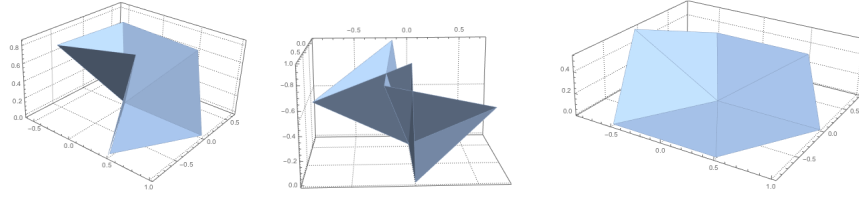


Figure 2: Hexagon configurations

where each value corresponds to a supplementary angle of a dihedral angle between two intersecting equilateral triangle planes affiliated with the hexagon, see Figure 1b.

The moduli space of the hexagon configuration collection is bounded by the hypercube $(\mathbb{R}/2\pi\mathbb{Z})^6$, with three degrees of freedom [4]. All origami hexagons belong to a three-parameter family.

2.2 Moduli space of deformations

In the context of **near flat configurations**, each dihedral angle between two adjacent triangle planes is close to π , thus each θ_i is close to zero.

By applying Taylor expansion and second order approximation, i.e., working in

$$\mathbb{Q}[\theta_i]/(\theta_i^2, \theta_i\theta_j), i \in \mathbb{Z}/6\mathbb{Z}, i \neq j,$$

we obtained an algebraic variety in \mathbb{R}^6 [4]. Reducing it into irreducible components, we change gear to another easier-to-understand algebraic variety Y ,

$$Y = \begin{cases} x_5^2 = x_2^2 + 2x_1x_2 + 2x_2x_3 + 2x_1x_3 \\ x_1 + x_2 = x_4 + x_5 \\ x_2 + x_3 = x_5 + x_6. \end{cases} \quad (1)$$

More importantly, each solution satisfying Y is a valid configuration and each near-flat hexagon's six fold angles is a 6-tuple point on Y .

Claim 1. *Algebraic variety Y is the moduli space of deformations of near-flat hexagon configurations.*

Proof. According to Chen and Santangelo, the space of deformations near the flat state is described by the null cone of some quadratic form [3]. For an origami hexagon, its moduli space has dimension 3. Thus we have such congruence,

$$\left\{ \begin{array}{l} \text{Configurations of} \\ \text{a near-flat hexagon} \end{array} \right\} \cong \left\{ \begin{array}{l} \text{Null cone of some quadratic} \\ \text{form } Q \text{ with dimension 3} \end{array} \right\} \quad (2)$$

Y is exactly described by the quadratic null cone inside \mathbb{R}^4 with actual dimension 3. We have showed that near-flat deformations are a subset of Variety Y . Then

$$\mathbb{R}^6 \supset V^4 \cong \mathbb{R}^4 \supset Y \cong \left\{ \begin{array}{l} \text{Null cone of some quadratic} \\ \text{form } Q \text{ with dimension 3} \end{array} \right\} \quad (3)$$

Combining Eq (2) and Eq (3),

$$Y \cong \left\{ \begin{array}{l} \text{Configurations of} \\ \text{a near-flat hexagon} \end{array} \right\},$$

we conclude that Y represents the moduli space of deformations near flat. \square

In the following context, we would refer Y as the hexagon configuration space (near flat). According to previous calculation [4], Y has the same topological shape as the quadratic form

$$x_1^2 + x_2^2 + x_3^2 - x_4^2 = 0,$$

which has signature $(3, 1)$. Y 's topological shape Y is described by a product of spheres, $S^2 \times S^0$.

3 Rational points on the hexagon configuration space

To characterize rational solutions of quadratic equations with rational coefficients, a geometric idea is to parametrize a line intersecting with a quadratic surface. There are two intersection points due to the fundamental theorem of algebra. Given a rational point O on a quadratic surface, we have such correspondence

$$\{\text{Rational lines through } O\} \cong \{\text{Rational points on this surface}\}.$$

Before diving into the rational points on the hexagon configuration space, we first examine the rational parametrization for the quadratic surface taking the form

$$W^2 = Y^2 + 2XY + 2YZ + 2XZ$$

It is a homogeneous form of

$$1 = y^2 + 2xy + 2yz + 2xz,$$

denoted as \mathcal{C} , with

$$x = \frac{X}{W}, y = \frac{Y}{W}, z = \frac{Z}{W}.$$

Suppose O is a rational point on \mathcal{C} , each rational line through O meets \mathcal{C} in two rational points, O and P . Conversely, each rational point P on \mathcal{C} could form a rational line by joining P to O . There is an one-to-one map from rational lines through O to all but one of the rational points on \mathcal{C} . To have a well-formed bijective map, we choose to work in projective space.

3.1 Interpretation of the projective space

Consider curve $\mathcal{C} : w^2 = y^2 + 2xy + 2yz + 2xz$ on projective space $P^3(\mathbb{R})$,

$$\mathcal{C} = \{[x : y : z : w] | w^2 = y^2 + 2xy + 2yz + 2xz\}.$$

With the substitution $v = x + z - y$, the curve takes the form

$$w^2 + x^2 + z^2 = v^2.$$

When $v = 0$, $(x, y, z, w) = (0, 0, 0, 0)$, there is no related point on $P^3(\mathbb{R})$.

When v is nonzero, it is equivalent to working in the affine space \mathbb{R}^3 . With convenient notations

$$a = \frac{x}{v}, c = \frac{w}{v}, b = \frac{z}{v},$$

we obtain

$$a^2 + b^2 + c^2 = 1,$$

which passes through $(1, 0, 0)$.

Given variables s, t , we have a rational line L passing through $(1, 0, 0)$ with the parametrization

$$L = \begin{cases} a - 1 = rm \\ b = sm \\ c = tm \end{cases}.$$

When $m = 0$, we have a solution $(1, 0, 0)$. When $m \neq 0$, m could be simplified as

$$m = \frac{-2r}{s^2 + t^2 - r^2}.$$

Then (a, b, c) takes the form

$$a = rm + 1 = \frac{s^2 + t^2 - r^2}{s^2 + t^2 + r^2}$$

$$b = sm = \frac{-2sr}{s^2 + t^2 + r^2}$$

$$c = tm = \frac{-2tr}{s^2 + t^2 + r^2}.$$

Tracing back, taking v as $s^2 + t^2 + r^2$, we have the parametrization

$$\begin{aligned} x &= s^2 + t^2 - r^2 \\ y &= 2r^2 + 2tr \\ z &= -2tr \\ w &= -2sr. \end{aligned}$$

In conclusion, all pairs (s, t, r) one-to-one correspond to all rational lines through $(1, 0, 0)$, thus they correspond to all rational points on the quadratic surface $w^2 = y^2 + 2xy + 2yz + 2xz$.

With the above parametrization, we have a well-formed bijection in $P^3(\mathbb{R})$ from points on $P^2(\mathbb{R})$ to rational points on the hexagon surface, i.e.

$$\{\text{All the points on } P^2(\mathbb{R})\} \cong \left\{ \begin{array}{c} \text{All the rational points on} \\ \mathcal{C} \text{ on } P^3(\mathbb{R}) \end{array} \right\}.$$

Claim 2. *The topological shape of the quadratic surface $w^2 = y^2 + 2xy + 2yz + 2xz$ on projective space $P^3(\mathbb{R})$ is a sphere.*

Proof.

$$w^2 = y^2 + 2xy + 2yz + 2xz \Leftrightarrow w^2 + x^2 + z^2 = (x + y + z)^2$$

If $w \neq 0$, this quadratic surface has the same topological shape as $y^2 - x^2 - z^2 = 1$ on \mathbb{R}^3 , which are two half sphere.

If $w = 0$, we are equivalently working in $P^2(\mathbb{R})$, $x^2 + z^2 = y^2$ has the shape as a circle. This circle is attached to each half sphere, resulting in a complete sphere. \square

Claim 3. *The topological shape of Y on $P^3(\mathbb{R})$ is S^2 .*

Proof. Y , as a subspace of \mathbb{R}^6 , has the same topological shape as $w^2 = y^2 + 2xy + 2yz + 2xz$, which is a subspace of \mathbb{R}^4 . This is because the map sending (x_1, \dots, x_6) in Y to $(w = x_1, y = x_4, x = x_3, z = x_5)$ is a continuous bijection, and the inverse function is also continuous. Claim 2 concludes that Y has the shape S^2 . \square

3.2 Rational parametrization

We want to find a bijective map from all the rational lines through some rational point on this hexagon surface to all rational points on the surface. Consider a 6-tuple $\theta_0 \in \mathbb{R}^6$, $\theta_0 = (\theta_1, \theta_2, \dots, \theta_6)$, $\theta_i \in \mathbb{R}$, satisfying

$$\theta_5^2 = \theta_2^2 + 2\theta_1\theta_2 + 2\theta_2\theta_3 + 2\theta_1\theta_3.$$

We have given out the rational parametrization for this quadratic form above as

$$\begin{aligned} \theta_1 &= s^2 + t^2 - r^2 \\ \theta_2 &= 2r^2 + 2tr \\ \theta_3 &= -2tr \\ \theta_5 &= -2sr. \end{aligned}$$

With two more linear constraints in Y

$$\begin{aligned} \theta_4 &= \theta_1 + \theta_2 - \theta_5 \\ \theta_6 &= \theta_2 + \theta_3 - \theta_5, \end{aligned}$$

we obtain the complete rational parametrization

$$\begin{aligned}\theta_1 &= s^2 + t^2 - r^2 \\ \theta_2 &= 2r^2 + 2tr \\ \theta_3 &= -2tr \\ \theta_4 &= s^2 + t^2 + 2tr + 2sr + r^2 \\ \theta_5 &= -2sr \\ \theta_6 &= 2r^2 + 2sr.\end{aligned}$$

Claim 4 (Real Solutions' Approachability). *For each real six-tuple $\theta = (\theta_1, \theta_2, \dots, \theta_6)$, $\theta_i \in \mathbb{R}$ on the hexagon surface, there exists a sequence $\{R_n\}$ satisfying Y that approaches θ .*

Proof. All the (s, t, r) -parametrization functions in \mathbb{R}^3 for θ are continuous, indicating for any real solution on the hexagon surface we could approach it with a rational solution sequence. \square

3.3 Flip operation

Observation 1. *If $(x, y, z) \in \mathbb{R}^3$ satisfies*

$$0 = Q(x, y, z) = y^2 + 2xy + 2xz + 2yz = 0,$$

then

$$0 = Q(2y + x, -y, 2y + z).$$

Points on the hexagon surface has the same transition invariant above. When we turn one mountain crease to a valley one with the same fold angle value, and add some specific values to its neighbors, the new point could still on this hexagon surface. We call this inter-set transformation the *flip operation*.

There are six natural *flip operations* on the space Y , corresponding to a local change at each of the six folds on the hexagon.

Definition 1. *A **flip operation** applied on a fold angle θ_i is a function*

$$F_i : \mathbb{R}^6 \rightarrow \mathbb{R}^6,$$

such that

$$\begin{aligned}\theta_{i-1} &\rightarrow \theta_{i-1} + 2\theta_i \\ \theta_{i+1} &\rightarrow \theta_{i+1} + \theta_i \\ \theta_i &\rightarrow -\theta_i\end{aligned}$$

$$F_i(\theta_1, \theta_2, \dots, \theta_6) = (\dots, \theta_{i-1} + 2\theta_i, -\theta_i, \theta_{i+1} + \theta_i, \dots)$$

In the vector space \mathbb{R}^6 , F_i is a linear map with matrix M_i ,

$$\begin{pmatrix} 1 & & & & & \\ & \ddots & & & & \\ & & 1 & 2 & & \\ & & & -1 & & \\ & & & 2 & 1 & \\ & & & & & \ddots \\ & & & & & & 1 \end{pmatrix}$$

For example, F_2 acts on configurations as shown in Figure 3.

Note that the inverse of F_i has the same matrix as M_i , thus $(F^{-1})_i = F_i$.

Proposition 1. *Suppose two six-tuples θ, γ are connected by a flip operation F_i , i.e. $F_i(\theta) = \gamma$.*

If θ is a valid hexagon configuration, i.e. satisfying variety Y , then γ satisfies Y .

Proof. This is directly deduced by Observation 1 and Claim 1. \square

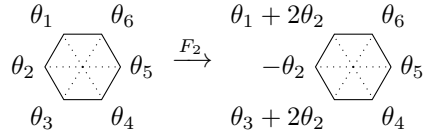


Figure 3: Flip operation

4 Integer points and the flip graph

Rational solutions are representing the practical crease angles, where it is natural to correspond rational points on the hexagon surface to physical configurations. The set of rational solutions measures near-flat configurations in external world. Intuitively, to reflect the internal relationships of near-flat configurations, we change gear to integer points on the hexagon surface. In the following context, we are studying primitive integer six-tuples $(\theta_1, \theta_2, \dots, \theta_6)$ satisfying Y ,

$$\theta_5^2 = \theta_2^2 + 2\theta_1\theta_2 + 2\theta_2\theta_3 + 2\theta_1\theta_3 \quad (4)$$

$$\theta_1 + \theta_2 = \theta_4 + \theta_5 \quad (5)$$

$$\theta_2 + \theta_3 = \theta_5 + \theta_6. \quad (6)$$

A noteworthy character for this set of integer configurations is that there doesn't exist any non-trivial 6-tuple with $\sum_i \theta_i = 0$. We would prove this later.

$\sum \theta_i$ is such an important character for a configuration that it deserves a name, **complexity**. We classify integer configurations by the sign of $\sum \theta_i$. Those with $\sum \theta_i > 0$ are described as having positive complexity, otherwise, negative complexity. There are some properties regarding to the partial sum of fold angles.

Proposition 2. *Suppose $(\theta_1, \theta_2, \dots, \theta_6)$ is a valid integer configuration with $\sum \theta_i > 0$, then*

$$(a). \theta_i + \theta_{i+1} \geq 0$$

$$(b). \theta_{i-1} + \theta_i + \theta_{i+1} > 0$$

$$(c). \theta_{i-1} + \theta_i + \theta_{i+1} \geq -2\theta_i$$

Proof. We will prove the second statement first.

(b). If there exists three consecutive angles with a non-positive sum, without loss of generality, suppose $\theta_1 + \theta_2 + \theta_3 \leq 0$. Adding $\theta_1^2 + \theta_3^2$ on both sides of Eq (4), we have

$$\theta_1^2 + \theta_3^2 + \theta_5^2 = (\theta_1 + \theta_2 + \theta_3)^2 \quad (7)$$

When $\theta_1 + \theta_2 + \theta_3 \leq 0$,

$$\theta_1 + \theta_2 + \theta_3 = \theta_3 + \theta_4 + \theta_5 = \theta_5 + \theta_6 + \theta_1 = -\sqrt{\theta_1^2 + \theta_3^2 + \theta_5^2}$$

Summing up $\theta_1 + \theta_2 + \theta_3$, $\theta_3 + \theta_4 + \theta_5$, and $\theta_5 + \theta_6 + \theta_1$, we add the rightmost term three times,

$$\sum \theta_i = -3\sqrt{\theta_1^2 + \theta_3^2 + \theta_5^2} - (\theta_1 + \theta_3 + \theta_5)$$

Since $a^2 + b^2 + c^2 \geq (a + b + c)^2/3$, we have the summation of all angles non-positive,

$$9(\theta_1^2 + \theta_3^2 + \theta_5^2) \geq (\theta_1 + \theta_3 + \theta_5)^2 \Rightarrow \sum \theta_i \leq 0,$$

which contradicts to the assumption. Thus $\theta_i + \theta_{i+1} + \theta_{i+2} > 0$, for any θ_i .

(a). [actually for this one, I forgot how to prove directly instead of using contradiction] Back to the first claim. If $\theta_i + \theta_{i+1} < 0$, without loss of generality, suppose $\theta_1 + \theta_2 < 0$, we have

$$\theta_1 + \theta_2 + \theta_3 = \pm\sqrt{\theta_1^2 + \theta_3^2 + \theta_5^2}.$$

Since we have proved that $\theta_1 + \theta_2 + \theta_3 > 0$,

$$\theta_1 + \theta_2 = \sqrt{\theta_1^2 + \theta_3^2 + \theta_5^2} - \theta_3 < 0$$

$$\Leftrightarrow \sqrt{\theta_1^2 + \theta_3^2 + \theta_5^2} < \theta_3 \Leftrightarrow \theta_1^2 + \theta_5^2 < 0,$$

which is a contradiction. Thus, $\theta_i + \theta_{i+1} \geq 0$.

(c). Without loss of generality, we could only check the case for $\theta_2 + 2\theta_3 + \theta_4 \geq -\theta_3$. Based on (b) and $a^2 + b^2 + c^2 \geq (a + b + c)^2/3$, we obtain

$$(\theta_1 + \theta_2 + \theta_3) + (\theta_3 + \theta_4 + \theta_5) = 2\sqrt{\theta_1^2 + \theta_3^2 + \theta_5^2} \geq \frac{2}{\sqrt{3}}(\theta_1 + \theta_3 + \theta_5) \geq \theta_1 + \theta_5 - \theta_3$$

$$\Leftrightarrow (\theta_2 + 2\theta_3 + \theta_4) + \theta_1 + \theta_5 \geq \theta_1 + \theta_5 - \theta_3$$

$$\Leftrightarrow \theta_2 + 2\theta_3 + \theta_4 \geq -\theta_3.$$

□

Notice that symmetrically, if $\sum \theta_i < 0$, we have $\theta_i + \theta_{i+1} \leq 0$ and $\theta_i + \theta_{i+1} + \theta_{i+2} < 0$.

Now, we could complete the proof of non-existence of a non-trivial configuration with zero complexity.

Proposition 3. *Any non-flat primitive integer 6-tuple $(\theta_1, \theta_2, \dots, \theta_6)$ satisfying Y has $\sum_i \theta_i$ either positive or negative.*

Proof. By Equation (7), if $\sum \theta_i = 0$,

$$9(\theta_1^2 + \theta_3^2 + \theta_5^2) = (\theta_1 + \theta_3 + \theta_5)^2$$

This equality only holds when $\theta_1 = \theta_3 = \theta_5$, but this will lead to a trivial solution, contradiction. □

Recall the flip operation we defined in Section 3.3. It is easy to see that flip operations won't change angles' parity. We claim that the sign of the complexity of a integer configuration would be preserved under flip operations.

Proposition 4. *For any two integer configurations connected by a flip operation described in Definition 1,*

$$(\theta_1, \theta_2, \dots, \theta_6) \xrightarrow{F_j} (\theta'_1, \theta'_2, \dots, \theta'_6).$$

$$(a) \sum \theta'_i = (\sum \theta_i) + 2\theta_j.$$

$$(b) \theta_i \equiv \theta'_i \pmod{2}.$$

$$(c) \text{ If } \sum \theta_i > 0, \text{ then } \sum \theta'_i > 0. \text{ Similarly, if } \sum \theta_i < 0, \text{ then } \sum \theta'_i < 0.$$

Proof. (a). Flipping angle θ_j , we have the transformation

$$\theta'_{j-1} = \theta_{j-1} + 2\theta_j$$

$$\theta'_j = -\theta_j$$

$$\theta'_{j+1} = \theta_{j+1} + 2\theta_j$$

$$\begin{aligned} \sum_i \theta'_i &= (\theta_{j-1} + 2\theta_j) + (-\theta_j) + (\theta_{j+1} + 2\theta_j) + \theta_{j+2} + \theta_{j+3} + \theta_{j+4} \\ &= \sum_j \theta_j + 2\theta_j = \sum_i \theta_i + 2\theta_j. \end{aligned}$$

(b). For the congruence classes mod 2,

$$\theta'_{j-1} \equiv \theta_{j-1} + 2\theta_j \equiv \theta_{j-1} \pmod{2},$$

where the case is same for θ_{j+1} .

$$\theta'_j = -\theta_j \equiv \theta_j \pmod{2}.$$

(c). We only need to consider the case when $\sum \theta_i > 0$.

$$\sum \theta'_i = (\sum \theta_i) + 2\theta_j = (\theta_{j-1} + 3\theta_j + \theta_{j+1}) + (\theta_{j+2} + \theta_{j+3} + \theta_{j+4})$$

By Proposition 2(b), $\theta_{j+2} + \theta_{j+3} + \theta_{j+4} > 0$, and by Proposition 2(c), $\theta_{j-1} + 3\theta_j + \theta_{j+1} \geq 0$, thus,

$$\sum \theta'_i > 0.$$

□

4.1 Flip graph

Creating graphs could provide a structural way to study a group. The Calkin-Wilf tree is an example ordering rational numbers.

Definition 2 (Calkin-Wilf Tree). *The Calkin-Wilf tree is rooted at integer 1, and any rational number expressed in simplest terms as the fraction $\frac{a}{b}$ has as its two children the numbers $\frac{a}{a+b}$ and $\frac{a+b}{b}$.*

As shown in Figure 4a, the Calkin-Wilf is determined by a root and a children generating rule. The fascinating property of the Calkin-Wilf tree is

Every positive rational number appears exactly once in the tree.

Definition 3 (Flip graph). *Analogous to the Calkin-Wilf tree, we defined the flip graph \mathcal{G} , which is an acyclic directed graph, as follows:*

1. \mathcal{G} is rooted at primitive integer configurations with only positive or only negative non-flat angles.
2. One primitive integer configuration $\theta \in \mathbb{Z}^6$, which is represented as a vertex in \mathcal{G} , has its children generated by flip operations with the following rules:
 - (a) when $\sum \theta_i > 0$, the children of θ are $\{F_i(\theta) | \forall \theta_i > 0\}$,
 - (b) when $\sum \theta_i < 0$, the children of θ are $\{F_i(\theta) | \forall \theta_i < 0\}$.

Considering rotations, there are six primitive integer configurations satisfying our definition for a valid root, which are the 3 rotations of $(0, 0, 1, 0, 0, 1)$ and 3 rotations of $(0, 0, -1, 0, 0, -1)$.

Claim 5. *Each vertex in the flip graph G corresponds to a valid primitive integer configuration.*

Proof. In \mathcal{G} , every root is a valid primitive integer configuration. All vertices are connected by a sequence of flip operations starting from a root. By Proposition 1, every vertex in \mathcal{G} must be a valid configuration on the hexagon surface.

For primitiveness, the flip operation F_i and its inverse F_i^{-1} are associated with the same integer matrix M_i , which preserves common factors of 6 angle values. Thus, any common angle value factor in \mathcal{G} should exist in the root. Thus, the configuration corresponding to each vertex is primitive and integral.

□

Figure 4b shows the first three layers of one component in the flip graph \mathcal{G} rooted with $(0, 0, 1, 0, 0, 1)$.

From now on, we will be working with the flip graph \mathcal{G} and all flip operations we refer to would be restricted to those defined in Definition 3 instead of general ones, i.e. the valid flip operation could only be applied to positive angles when the hexagon complexity is positive.

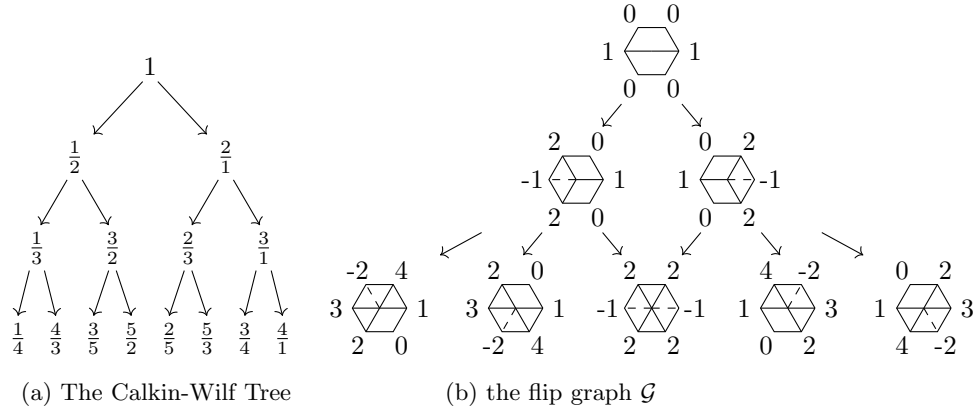


Figure 4: The Calkin-Wilf Tree and Integer configuration flip graph

Proposition 5. Suppose $\mathcal{P} = (\theta_1, \dots, \theta_6)$ is a valid primitive integer configuration with $\sum \theta_i > 0$. It has child $\mathcal{C} = (\theta'_1, \dots, \theta'_6)$ by flipping positive fold angle θ_j . Then

- (a) $|\theta'_i| \geq |\theta_i|$.
- (b) $|\theta'_{j+1}| \geq |\theta_j|, |\theta'_{j-1}| \geq |\theta_j|$.
- (c) θ_j is unique, i.e. $\nexists k$ s.t. $F_k(\mathcal{P}) = \mathcal{C}, k \neq j$.

Proof. (a). We only need to check θ'_{j+1} . By Proposition 2(a), $\theta_j + \theta_{j+1} \geq 0$. Since a flip operation is acting on the positive angle, $\theta_j > 0$. Then by $|a + b| = |a| + |b|$, when $a, b > 0$,

$$|\theta'_{j+1}| = |\theta_{j+1} + 2\theta_j| = |\theta_{j+1} + \theta_j| + |\theta_j| \geq |(\theta_{j+1} + \theta_j) - \theta_j| = |\theta_j|.$$

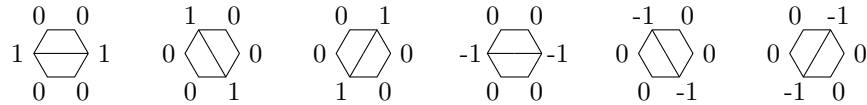
(b). It is sufficient to check θ'_{j+1} only. With the same reason above, $\theta_j + \theta_{j+1} > 0, \theta_j > 0$, we have

$$|\theta'_{j+1}| = |\theta_{j+1} + 2\theta_j| = |\theta_{j+1} + \theta_j| + |\theta_j| \geq |\theta_j|.$$

(c). Prove by contradiction. Suppose there exists k satisfying the above condition. Then in \mathcal{P} , $\theta_k > 0$ and in \mathcal{C} , $\theta'_k < 0$. However, \mathcal{C} is generated by \mathcal{P} by flipping θ_j , which could not make any angle positive except θ'_j . It is contradicted to the transition from positive θ_k to negative θ'_k . \square

Claim 6. The flip graph \mathcal{G} consists of six isomorphic connected components.

Proof. Based on the definition of \mathcal{G} , we have all roots with the following configuration:

Figure 5: Roots for Flip Graph \mathcal{G}

In Proposition 5a, if $\sum \theta_i > 0$, the flip operation is defined on a positive angle, thus $\sum \theta'_i > 0$. Then we could conclude that all configurations generated from the one of the positive roots must have positive complexity. The same situation applies to negative roots. Then each vertex in \mathcal{G} connected to a positive root cannot have a path to any negative root. We have two components so far.

Now let's consider the configurations reached by all the positive roots. From Proposition 5b, the angles' parity are the same if two vertices are connected, which shows every vertex connected to

the root $(0, 0, 1, 0, 0, 1)$ is not connected to $(0, 1, 0, 0, 1, 0)$, as well as $(1, 0, 0, 1, 0, 0)$. Thus, there are three connected components rooted from one of the positive roots.

In conclusion, each root in Figure 5 is in a connected component of \mathcal{G} and all those components are isolated to each other. Since those roots are isomorphic to each other, the rest of the subgraph connected by flip operations in \mathcal{G} makes six components isomorphic. \square

Since six components are isomorphic, it is sufficient to study one piece, which is rooted at $(0, 0, 1, 0, 0, 1)$, denoted as \mathcal{D} .

Claim 7. *Graph \mathcal{D} has the following properties:*

(a) \mathcal{D} is acyclic.

(b) \mathcal{D} is graded.

Proof. (a). Since the complexity in \mathcal{D} is increased by each flip, there is no flip operation sequence that could visit a configuration twice. So \mathcal{D} has no directed cycle.

(b). The distance from one vertex to the root is consistent for different generating paths. \square

To make the flip graph \mathcal{G} capable of revealing the structure of primitive integer configurations, we are interested in the correspondence between primitive integer configurations and vertices in \mathcal{G} . Like how the Calkin-Wilf tree is introduced, we expect the flip graph \mathcal{G} performances similarly – containing a one-to-one correspondence between vertices and configurations.

With those angles sum properties in Proposition 2, we could prove that each primitive configuration must show up in the flip graph \mathcal{G} . Equivalently, each primitive integer configuration is reached by a sequence of valid flip operations from a root configuration in Figure 5.

Claim 8. *Every integer configuration $(\theta_1, \theta_2, \dots, \theta_6)$ with $\sum \theta_i > 0$ and $\gcd(\theta_1, \theta_2, \dots, \theta_6) = 1$, is reached by one of the positive roots, i.e. three rotations of $(0, 0, 1, 0, 0, 1)$.*

Proof. Consider any primitive integer configuration θ with positive complexity. All the possible mountain-valley labellings for a valid hexagon is shown in Figure 6, according to [4].

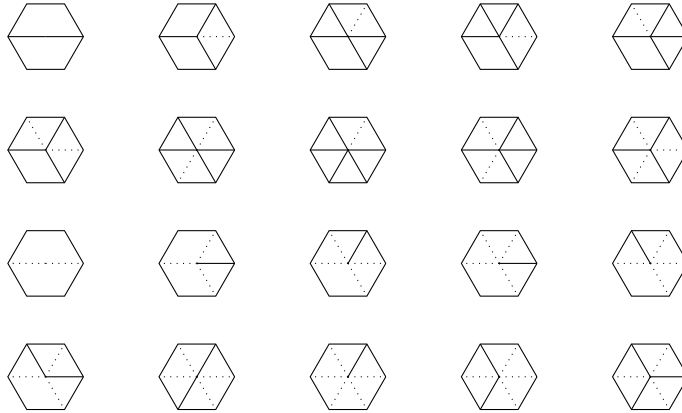


Figure 6: Mountain-valley labellings

If θ is a root, then it is in the flip graph \mathcal{G} .

If θ is not a root, then it must have a negative angle. Recursively applying the general flip operation on θ 's negative angle, there are only two possibilities:

- to generate a finite path with the end point as one of three rotations of $(0, 0, 1, 0, 0, 1)$,
- to generate an infinite path – visit infinite primitive configurations (consider repetitive visit)

If the path generated by negative flip operations is finite, consider the last primitive configuration γ on this path. If γ is a root, it falls under Case a. If γ is not a root, then it must have a negative angle which could reach a new primitive configuration. This contradicts γ being the last one in this path.

By Proposition 2(c), the general flip operation would preserve the sign of complexity. Here recursive flip operation is applied on negative angles, so the complexity is progressively decreasing. In that case the path could not revisit any configuration nor form an infinite path. So, Case b is impossible when applying negative flip operation.

Now, under the condition, for any integer primitive configuration we could find a finite path from it to one of the roots by applying the flip operation on negative angles. While considering the inverse direction, each integer primitive configuration must be reached by one of the roots by the flip operation applying on positive angles, which is exactly what we defined in the flip graph \mathcal{G} . \square

Now, we reach an analogue to the Calkin-Wilf tree.

Claim 9 (Analogue to the Calkin-Wilf tree). *Primitive integer configurations on the hexagon surface correspond one-to-one to the vertices in the flip graph \mathcal{G} , considering rotations and reflections.*

Proof. This is directly deduced by Claim 5 and Claim 8. \square

4.2 Mountain-valley classification

We gave out closed formula for the number of vertices on each level and the number of mountain-valley configurations among them. By generating the Markov transition matrix, we calculated the limiting distribution for mountain-valley configurations.

According to Proposition 2 and Claim 9, configurations with positive complexity could not contain two consecutive negative fold angles. They must have the following configurations in Figure 7 up to rotations.

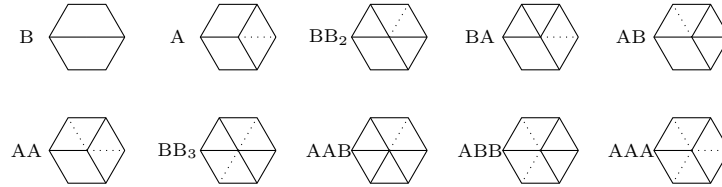


Figure 7: Mountain-valley labellings with positive complexity

Given a mountain-valley type, the children generated in Flip Graph are certain, shown in Figure 8. Based on the mountain-valley transition relations, in the perspective of Markov transition process, the column-stochastic transition matrix for 3-dimensional configurations BB_3, AAB, ABB, AAA is

$$\begin{array}{ccccc}
 & BB_3 & AAB & ABB & AAA \\
 BB_3 & 0 & 0.2 & 0.5 & 1.0 \\
 AAB & 0 & 0.4 & 0.25 & 0 \\
 ABB & 1.0 & 0.4 & 0 & 0 \\
 AAA & 0 & 0 & 0.25 & 0
 \end{array} ,$$

with eigenvector $v = \begin{bmatrix} 0.33 \\ 0.17 \\ 0.4 \\ 0.1 \end{bmatrix}$ corresponding to the dominant eigenvalue $\lambda = 1$. Thus the final distribution for those mountain-valley configurations is consistent with v .

Claim 10. *The 3-dimensional areas' ratio in the null cone of [4] is*

$$BB_3 : AAB : ABB : AAA = 0.33 : 0.17 : 0.4 : 0.1.$$

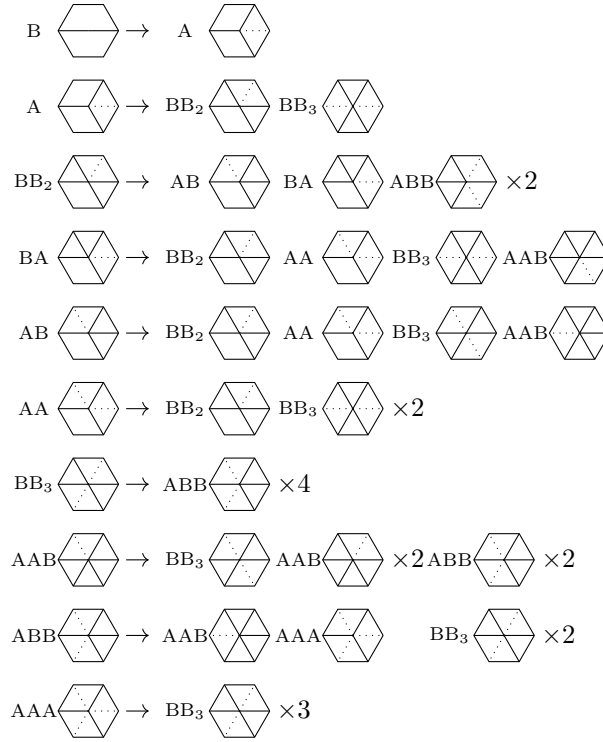


Figure 8: Flip images of configurations with positive complexity

Consider the isolated component \mathcal{D} with the root $(1, 0, 0, 1, 0, 0)$. Recall Claim 7, Graph \mathcal{D} is graded. As a result, we could group nodes by layers, where

$$\{\text{nodes on Layer } n\} = \{\text{nodes which need } n \text{ flips to reach a root node}\}.$$

Mountain-valley configuration is a good tool to help classifying vertices on Graph \mathcal{D} . We have discussed how flip operation works on mountain-valley configurations. Since \mathcal{D} is determined by roots and flip operation, we could calculate the number of vertices on each layer by discussing different mountain-valley configurations separately.

In the following context, we will focus on 3-dimensional configurations BB_3, AAB, ABB, AAA on each layer.

Let

$$\text{type}(n) = \#\{\text{nodes of type on layer } n\}, \text{ where type} = BB_3, AAB, ABB, \text{ or } AAA.$$

To go from layer n to layer $n+1$, the number of children nodes is determined by mountain-valley type, as well as mountain-valley type of children. Also, some children are counted multiple times, because they have more than one parent node.

Proposition 6. *Each configuration in the graph \mathcal{D} has k parents, where k is the number of negative fold angles it has.*

Proof. By doing the inverse flip operation of a negative angle in a configuration \mathcal{C} , we could generate another node in \mathcal{D} , denoted by \mathcal{P} . By how we defined parent-child relationship in Definition 3, \mathcal{P} must be a valid parent for \mathcal{D} . Most importantly, according to Proposition 5(c), all the parent nodes \mathcal{C} reached would not overlap. Thus the number of negative angles in \mathcal{C} indicates the number of parents it has in graph \mathcal{D} . \square

$$\begin{aligned}
 \# \{ \text{children in layer } n+1 \} &= \begin{pmatrix} 2_{BB_3}(n+1) \\ AAB(n+1) \\ 2_{ABB}(n+1) \\ 3_{AAA}(n+1) \end{pmatrix} = \begin{pmatrix} 0 & 1 & 2 & 3 \\ 0 & 2 & 1 & 0 \\ 4 & 2 & 0 & 0 \\ 0 & 0 & 1 & 0 \end{pmatrix} \begin{pmatrix} BB_3(n) \\ AAB(n) \\ ABB(n) \\ AAA(n) \end{pmatrix} \\
 &\Rightarrow \begin{pmatrix} BB_3(n+1) \\ AAB(n+1) \\ ABB(n+1) \\ AAA(n+1) \end{pmatrix} = \begin{pmatrix} 0 & 1/2 & 1 & 3/2 \\ 0 & 2 & 1 & 0 \\ 2 & 1 & 0 & 0 \\ 0 & 0 & 1/3 & 0 \end{pmatrix} \begin{pmatrix} BB_3(n) \\ AAB(n) \\ ABB(n) \\ AAA(n) \end{pmatrix}
 \end{aligned}$$



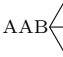
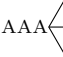





Figure 9: Transitions among 3-dimensional configurations

Claim 11. *The layer-counting transition matrix for 3-dimensional configurations is*

$$\begin{bmatrix} 0 & 1/2 & 1 & 3/2 \\ 0 & 2 & 1 & 0 \\ 2 & 1 & 0 & 0 \\ 0 & 0 & 1/3 & 0 \end{bmatrix}.$$

More generally, if we consider all the mountain-valley types in Figure 7, we have the general layer-counting transition matrix H as

$$H = \begin{bmatrix} 0 & 0 & 0 & 0 & 0 & 0 & 0 & 0 & 0 & 0 \\ 1 & 0 & 0 & 0 & 0 & 0 & 0 & 0 & 0 & 0 \\ 0 & 1 & 0 & 1 & 1 & 1 & 0 & 0 & 0 & 0 \\ 0 & 0 & 1 & 0 & 0 & 0 & 0 & 0 & 0 & 0 \\ 0 & 0 & 1 & 0 & 0 & 0 & 0 & 0 & 0 & 0 \\ 0 & 0 & 0 & 1 & 1 & 0 & 0 & 0 & 0 & 0 \\ 0 & 1/2 & 0 & 1/2 & 1/2 & 1 & 0 & 1/2 & 1 & 3/2 \\ 0 & 0 & 0 & 1 & 1 & 0 & 0 & 2 & 1 & 0 \\ 0 & 0 & 1 & 0 & 0 & 0 & 2 & 1 & 0 & 0 \\ 0 & 0 & 0 & 0 & 0 & 0 & 0 & 0 & 1/3 & 0 \end{bmatrix}$$

Proposition 7. *The number of nodes in each layer has growing speed $O(t^n)$, where t is the dominant eigenvalue for H , $t = 1 + \sqrt{3}$.*

5 Pythagorean 4-tuples

In the proof of Proposition 2, an equivalent transformation is noteworthy:

$$Y \cong \begin{cases} x_1^2 + x_3^2 + x_5^2 = (x_1 + x_2 + x_3)^2 \\ x_1 + x_2 = x_4 + x_5 \\ x_2 + x_3 = x_5 + x_6 \end{cases}.$$

If we set $r = x_1 + x_2 + x_3$, then (x_1, x_3, x_5, r) satisfying $x_1^2 + x_3^2 + x_5^2 = r^2$ uniquely determines a valid hexagon configuration with parametrization

$$\begin{aligned} x_1 &= x_1 \\ x_3 &= x_3 \\ x_5 &= x_5 \\ x_2 &= r - x_1 - x_3 \\ x_4 &= r - x_3 - x_5 \\ x_6 &= r - x_1 - x_5. \end{aligned}$$

When considering integer configurations, Pythagorean 4-tuples should be gazed.

Definition 4 (Pythagorean 4-tuples). (x_1, x_2, x_3, x_4) is a (*primitive*) Pythagorean 4-tuple if x_1, x_2, x_3, x_4 are integers satisfying

$$x_1^2 + x_2^2 + x_3^2 = x_4^2, \quad \gcd(x_1, x_2, x_3, x_4) = 1, \quad \text{and} \quad x_4 > 0.$$

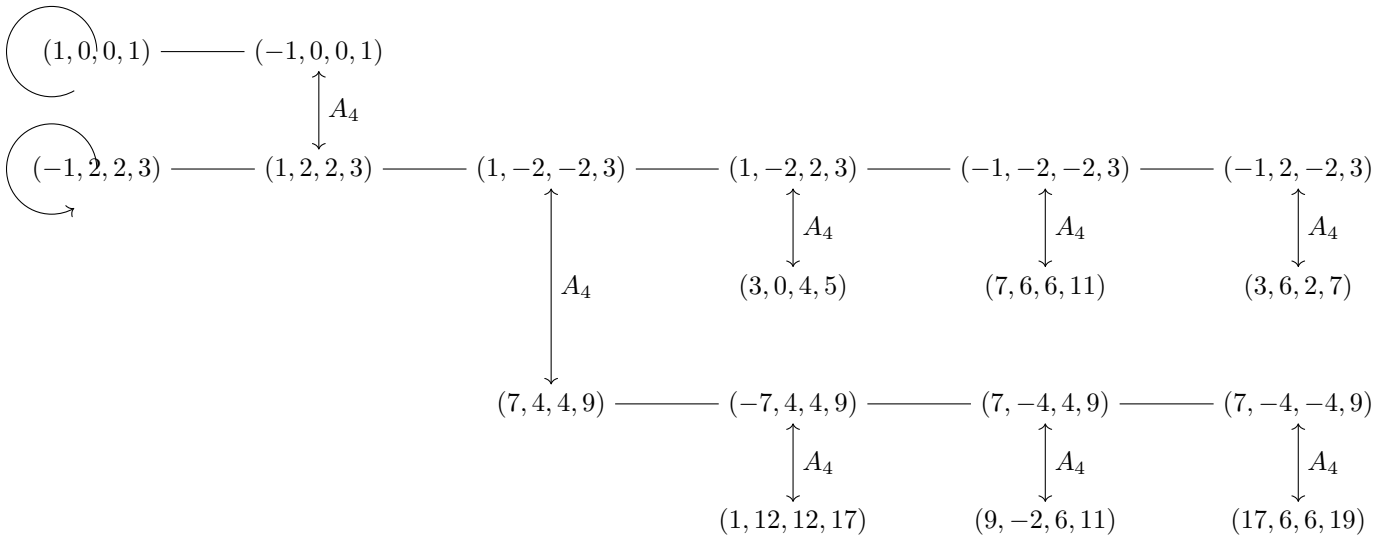
According to Cass and Arpaia [2], on Pythagorean 4-tuples, there is an action characterized by the composition of sign changes and the matrix A_4

$$A_4 = \begin{bmatrix} 0 & -1 & -1 & 1 \\ -1 & 0 & -1 & 1 \\ -1 & -1 & 0 & 1 \\ -1 & -1 & -1 & 2 \end{bmatrix},$$

which generates other complicated Pythagorean 4-tuples from simpler ones. For example, A_4 could send $(3, -2, -6, 7)$ to $(15, 10, 6, 19)$,

$$\begin{pmatrix} 0 & -1 & -1 & 1 \\ -1 & 0 & -1 & 1 \\ -1 & -1 & 0 & 1 \\ -1 & -1 & -1 & 2 \end{pmatrix} \begin{pmatrix} 3 \\ -2 \\ -6 \\ 7 \end{pmatrix} = \begin{pmatrix} 15 \\ 10 \\ 6 \\ 19 \end{pmatrix}$$

5.1 Pythagorean graph



5.2 Connection to hexagon configuration

For one hexagon configuration $(\theta_1, \theta_2, \dots, \theta_6)$, it has two representations in terms of Pythagorean 4-tuples: $(\theta_1, \theta_3, \theta_5, r_{\text{odd}})$ and $(\theta_2, \theta_4, \theta_6, r_{\text{even}})$.

$$(\theta_1, \theta_3, \theta_5, r_{\text{odd}}) \leftrightarrow \begin{array}{c} r_{\text{odd}} - \theta_1 - \theta_3 \quad \theta_1 \\ \theta_3 \quad \text{hexagon} \quad r_{\text{odd}} - \theta_1 - \theta_5 \\ r_{\text{odd}} - \theta_3 - \theta_5 \quad \theta_5 \end{array} \quad (8)$$

$$(\theta_2, \theta_4, \theta_6, r_{\text{even}}) \leftrightarrow \begin{array}{c} \theta_2 \quad r_{\text{even}} - \theta_6 - \theta_2 \\ r_{\text{even}} - \theta_4 - \theta_2 \quad \text{hexagon} \quad \theta_6 \\ \theta_4 \quad r_{\text{even}} - \theta_4 - \theta_6 \end{array} \quad (9)$$

The Pythagorean tuples in (8) and (9) are related by matrix A_4 .

More explicitly, if we set (a, b, c, r) as a representation of a configuration, then the other equivalent representation would be $(r - b - c, r - a - c, r - a - b, 2r - a - b - c)$, which is obtained by rotating the first configuration by 180 degree. Those two 4-tuple representations are connected by A_4 .

Now we only consider odd-angle representation. For a pythagorean 4-tuple (a, b, c, r) , we define the corresponding hexagon configuration as $(\theta_1 = a, \theta_2 = r - a - b, \theta_3 = b, \theta_4 = r - b - c, \theta_5 = c, \theta_6 = r - a - c)$.

Theorem 2. *Under the odd-angle representation, there is a bijection between primitive pythagorean 4-tuples and primitive integer hexagon configurations.*

5.2.1 Flip operation

We denote a sign change operation on pythagorean group as s_{2i-1} if it is changing the sign of the x_i .

If we apply a sign change s_k on the pythagorean 4-tuple, we have a corresponding Flip operation F_k on the hexagon configuration with odd angles θ_1, θ_3 , or θ_5 . If we have a composition of $A_4 \circ s_k \circ A_4$, then the corresponding transition in hexagon configuration is flipping a even angle, i.e. $\theta_2, \theta_4, \theta_6$. More specifically, we have $A_4 \circ s_k \circ A_4$ correspond to $F_{(k+3) \bmod 6}$. See an example in Figure 10.

The bijection map on the flip graph \mathcal{G} also reveals the structure of pythagorean 4-tuples. Consider a 4-tuple set $\mathcal{R} = \{(1, 0, 0, 1), (0, 1, 0, 1), (0, 0, 1, 1)\}$.

Claim 12. *Every pythagorean primitive 4-tuple could be reached by one element of \mathcal{R} if they have the same parity.*

5.2.2 Pythagorean graph \mathcal{H} and hexagon flip graph \mathcal{G}

To give out a simpler statement about the connection between Pythagorean 4-tuple and hexagon configuration, we define a graph \mathcal{H} containing operations and 4-tuples as follows:

Definition 5 (Restricted graph). *In graph \mathcal{H} , the primitive 4-tuple $(1, 0, 0, 1)$, denoted as r , is a node in $V(\mathcal{H})$. If a pythagorean 4-tuple is generated by the composition of a sequence of operations s_i and A_4 , it is representing a node in $V(\mathcal{H})$. s_i will only change **one** element's sign and could only be applied to a positive value.*

The hexagon flip graph \mathcal{G} and the Pythagorean 4-tuple graph \mathcal{H} can be related by constructing a graph \mathcal{K} which has graph-theoretic maps $\mathcal{K} \rightarrow \mathcal{G}$ and $\mathcal{K} \rightarrow \mathcal{H}$.

The graph \mathcal{K} has twice as many vertices as \mathcal{G} and \mathcal{H} , in the sense that $\mathcal{K} \rightarrow \mathcal{G}$ and $\mathcal{K} \rightarrow \mathcal{H}$ are 2-to-1 on vertices. (\mathcal{G} and \mathcal{H} have the “same number” of vertices, i.e. there are two natural bijections between vertices of \mathcal{G} and vertices of \mathcal{H} , the odd-angle and even-angle maps.)

The relation to get from \mathcal{G} to \mathcal{K} is replacing each vertex with an edge and two vertices.

The relation to get from \mathcal{H} to \mathcal{K} is known as a “double cover” (or “degree 2 cover”).

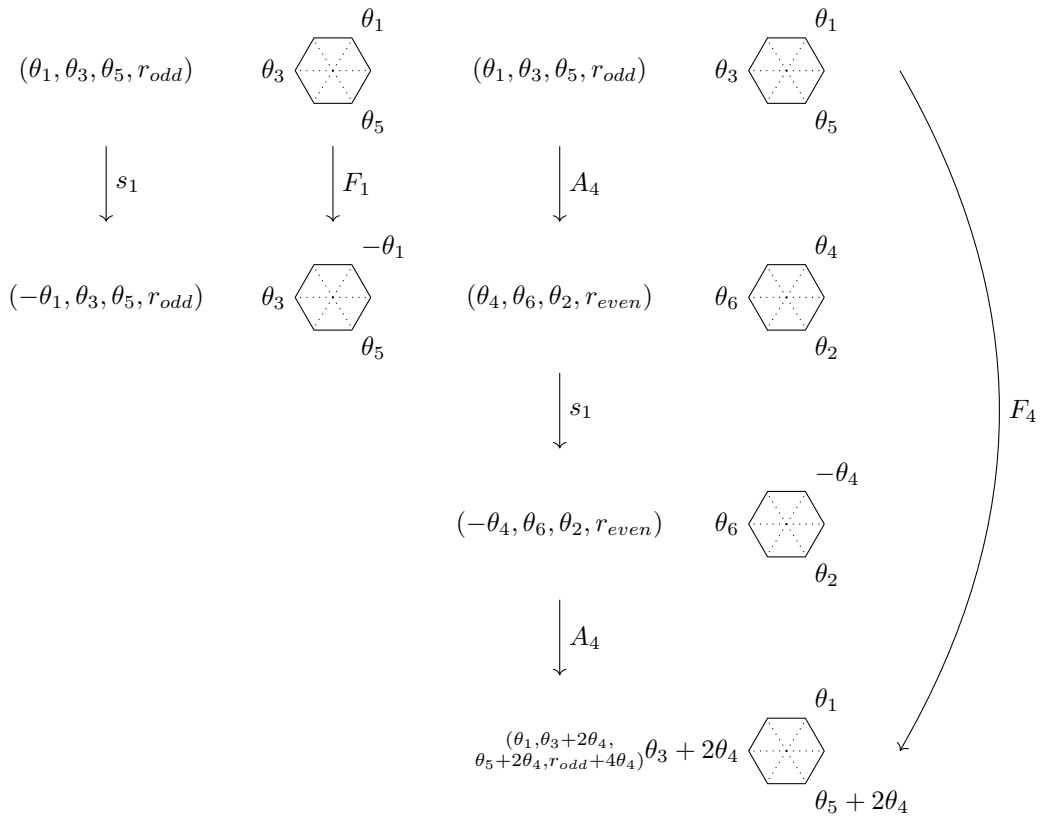


Figure 10: Operations correspondence between Pythagorean 4-tuple and hexagon configuration

References

- [1] D. J. BALKCOM AND M. T. MASON, *Robotic origami folding*, The International Journal of Robotics Research, 27 (2008), pp. 613–627.
- [2] D. CASS AND P. J. ARPAIA, *Matrix generation of pythagorean n -tuples*, Proceedings of the American Mathematical Society, 109 (1990), pp. 1–7.
- [3] B. G.-G. CHEN AND C. D. SANTANGELO, *Branches of triangulated origami near the unfolded state*, Physical Review X, 8 (2018), p. 011034.
- [4] A. CUZA, Y. LIU, AND O. SAEED, *Origami on lattices*, (2019).
- [5] G. DARBOUX, *De l'emploi des fonctions elliptiques dans la théorie du quadrilatère plan*, Bulletin des Sciences Mathématiques et Astronomiques, 2e série, 3 (1879), pp. 109–128.
- [6] I. IZMESTIEV, *Four-bar linkages, elliptic functions, and flexible polyhedra*, Computer Aided Geometric Design, 79 (2020), p. 101870.
- [7] M. F. LARRY L. HOWELL, ROBERT J. LANG AND R. J. WOOD, *Special issue: Folding-based mechanisms and robotics*, J. Mechanisms Robotics, 8(3) (2016), p. 030301.